

# **SIMULATION STUDIES OF AN ENERGY DETECTION SCHEME FOR MOBILE RADIO CHANNEL**

*A Thesis submitted  
in partial fulfilment of the Requirements  
for the degree of*

**MASTER OF TECHNOLOGY**

*By*

**ADITYA TRIVEDI**

*To the*

**DEPARTMENT OF ELECTRICAL ENGINEERING  
INDIAN INSTITUTE OF TECHNOLOGY KANPUR**

*March 1997*

0 2 APR 1997 / E E

CLARK  
PUR

No. **A** 123287

997- M-TRI-SIM

## CERTIFICATE

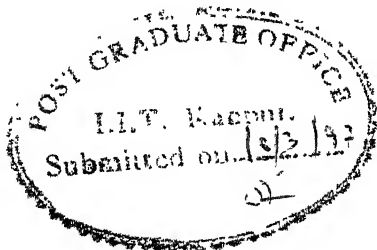
This is to certify that the work contained in the thesis entitled 'SIMULATION STUDIES OF AN ENERGY DETECTION SCHEME FOR MOBILE RADIO CHANNEL' by ADITYA TRIVEDI has been carried out under my supervision and that this work has not been submitted elsewhere for a degree.



March, 1997

Dr. P. K. CHATTERJEE  
Professor

Department of Electrical Engineering  
Indian Institute of Technology  
Kanpur



## ABSTRACT

Intersymbol interference (ISI) is one of the major problems encountered in cellular mobile radio communication. In presently used mobile systems channel equalization is used which results in complex receiver design. To avoid the resulting complexities an energy detection scheme has been proposed. Simulation of an energy detection scheme using binary Frequency Shift Keying (FSK) as the modulation technique has been carried out. Data rate used in the simulation is the same as used in GSM system. Multipath spread or mean-square delay spread is taken as  $4.6 \mu\text{sec}$ . as reported in literature. Probability of error has been calculated for different SNR values and for three different IF bandwidths.

For  $10^{-3}$  probability of error SNRs are found to be 18.5 dB, 19 dB, and 21 dB (approximately) for  $2/T$ ,  $1.5/T$ , and  $1/T$  IF bandwidth respectively.

## ACKNOWLEDGEMENT

I wish to express my heartfelt reverence and gratitude to Prof. P. K. Chatterjee for his able guidance, valuable suggestions and patience during the course of this study.

I wish to thank Dr. Sumana Gupta for allowing me to work in DSP Lab.

I sincerely acknowledge the help of Mr. Yash Pal for the painstaking effort in typing the manuscript.

The goodwill and support of my friends Samir, M. L. Singh, Gaurav Raghuvanshi was also a great asset to me during my stay at IIT Kanpur.

I am greatly indebted to my family members who always encouraged and held me in high spirits.

Finally, I gratefully acknowledge Madhav Institute of Technology & Science, Gwalior for providing me an opportunity to pursue a Master's Degree at IIT Kanpur.

**ADITYA TRIVEDI**

## CONTENTS

	Page No
List of Figures	
Abstract	
CHAPTER - 1 INTRODUCTION	1
1.1 CELLULAR MOBILE COMMUNICATION	1
1.2 DIGITAL MOBILE COMMUNICATION SYSTEMS	2
1.2.1 GSM	2
1.2.2 IS (Interim Standard ) - 54	2
1.2.3 Personal Digital Cellular (PDC) System	3
1.2.4 IS (Interim Standard) - 95	3
1.2.5 DECT (Digital European Cordless Telecommunication)	4
1.3 PROBLEMS IN MOBILE COMMUNICATION	4
1.4 CHANNEL EQUALIZATION	5
1.5 ENERGY DETECTION	7
1.6 STATEMENT OF THE PROBLEM	7
1.7 THESIS LAYOUT	8
CHAPTER - 2 FADING CHANNELS	9
2.1 GENERAL FADING CHANNEL MODEL	10
2.1.1 Rayleigh and Rician Fading Channels	12
2.1.2 Correlation Functions	13
2.2 WSSUS FADING CHANNELS	14
2.3 DOUBLY SPREAD CHANNELS	16
2.4 TIME-SELECTIVE FADING CHANNELS	18

	2.5	FREQUENCY-SELECTIVE FADING CHANNELS	22
	2.6	NONDISPERSIVE FADING CHANNELS	23
CHAPTER - 3		CHARACTERIZATION OF THE MOBILE RADIO CHANNEL	25
	3.1	TIME-SELECTIVE FADING	25
	3.2	FREQUENCY-SELECTIVE FADING	28
	3.3	MOBILE RADIO PATH LOSS	31
	3.4	SHADOWING	31
CHAPTER - 4		SIMULATION OF FSK ENERGY DETECTION MOBILE SYSTEM	33
	4.1	Energy Detection	33
	4.2	Simulation of Energy Detection Scheme	36
	4.2.1	Tapped Delay Line model of the Channel	36
	4.2.2	Signal Flow Diagram	40
	4.2.3	Simulation Details	42
	4.3	SIMULATION RESULTS	43
	4.4	DISCUSSION OF THE RESULTS	43
CHAPTER - 5		CONCLUSION	45
	5.1	SUGGESTION FOR FUTURE WORK	45
REFERENCES			47

## LIST OF FIGURES

	Page No
Fig. 2.1 Propagation model of a general fading channel	11
Fig. 2.2 Effect of transmitting a pulse over a time-selective fading channel	21
Fig. 2.3 Effect of transmitting a pulse over a frequency-selective fading channel	21
Fig. 2.4 Summary of hierarchy of fading channel models	24
Fig. 3.1 Typical Rayleigh Fading at 845 MHz	27
Fig. 3.2 Plot of Doppler Spectrum for a mobile radio channel	27
Fig. 3.3 Average Power Delay profiles	30
Fig. 4.1 Energy detection FSK System	35
Fig. 4.2 3-Frequency-Pair FSK Signaling Sequence	35
Fig. 4.3 Average Power Delay Profile for suburban and urban areas (in absolute scale)	37
Fig. 4.4 Tapped Delay Line Channel Model	39
Fig. 4.5 Signal Flow Diagram of the Simulated System	41
Fig. 4.6 Measured Error Probability of the Simulated System	44



# CHAPTER - 1

## INTRODUCTION

1

### 1.1 CELLULAR MOBILE COMMUNICATION

To meet the increasing demand of mobile communication large capacity systems are needed. Conventional mobile telephone systems are not suitable for this purpose because of limited service capability, poor service performance and inefficient frequency spectrum utilization [1]. As a result it is often necessary to use cellular systems, where many fixed radio base stations are built and the same frequency is reused in different cells. A geographical area is divided into smaller hexagonal shape areas, called cells. The spectral efficiency of the system is increased by a factor equal to the number of times a frequency may be reused within a geographical area. A basic cellular system consists of three parts : a mobile unit, a cell site or base station and a mobile telephone switching office (MTSO).

A mobile telephone unit contains a transreceiver, a control unit and antenna system. The base station provides interface between the MTSO and the mobile units. It consists of control unit, antennas, data terminals, etc. MTSO, the central coordinating element for all base stations contains the cellular processor and cellular switch. It interfaces with telephone company zone offices, control call processing like handoffs, etc. and handle billing activities. Communication with a mobile in a given cell is made to the base station that serves the cell. Direct mobile-to-mobile communication is not permitted in the

## 1.2 DIGITAL MOBILE COMMUNICATION SYSTEMS

This section gives brief specifications of the various mobile systems currently in use.

### 1.2.1 GSM

Global System for Mobile Communications (GSM) has been deployed commercially throughout Europe. GSM forward band (i.e., Base to mobile transmission) is from 935 MHz to 960 MHz and the reverse band (i.e., Mobile to base transmission) is from 890 MHz to 915 MHz. RPE-LPC/LTP (residual pulse excited, linear prediction coder with long-term prediction) speech coder is used at 13 kbps. Rate-1/2 convolution codes are used for channel coding. GSM carrier spacing is at 200 KHz. Eight voice channels are time multiplexed on one carrier [2,3]. In all 1000 voice channels can be accommodated simultaneously. The gross (channel) bit rate is 270.8 kbps. Modulation technique used is GMSK (Gaussian minimum shift keying). The modulation efficiency is 1.35 bps/Hz. Adaptive equalizer using Viterbi algorithm is used for reliable signal detection. The most prominent characteristic of the GSM physical layer is the elaborate timing structure. Slow frequency hopping (SFH) at the rate of 217 hops per second is employed.

### 1.2.2 IS (Interim Standard) - 54

This system has been deployed in US and Canada. The IS-54 has a total bandwidth of 50 MHz, same as for GSM. The forward band is from 869 MHz to 894 MHz and the reverse band from 824 MHz to 849 MHz. The carrier spacing of IS-54 is 30 KHz, same as in

the first generation AMPS (Advanced Mobile Phone Service) system. Each digital channel operates at 48.6 kbps carrying three user signals. Adaptive equalizer is needed. The modulation method used is  $\pi/4$  shifted differentially encoded quadrature phase shift keying. ( $\pi/4$ -DQPSK). The modulation efficiency is 1.62 bps/Hz, a 20 percent improvement over GSM. The main penalty of linear modulation is power efficiency [3,4]. The speech coding technique adopted is vector-sum excited linear prediction (VSELP) with the rate of 7.95 kbps. Rate-1/2 convolution code is used for channel coding.

#### 1.2.3 Personal Digital Cellular (PDC) System

This is being used in Japan. Total bandwidth allotted is 32 MHz, 16 MHz each for forward band and reverse band. The PDC has a carrier spacing of 25 KHz. It has 3 voice channels per carrier. Modulation technique used is  $\pi/4$ -DQPSK. To avoid extreme complexity in the power amplifier the gross (channel) bit rate is chosen to be 42 kbps, producing a higher modulation efficiency of 1.68 kbps/Hz [4,5]. Access method used is TDMA, same as used for GSM and IS-54. Speech coder used is VSELP at 6.7 kbps. Rate-1/2 convolution code is used for channel coding. Equalizer is optional.

#### 1.2.4 IS (Interim Standard) - 95

As proposed by Qualcomm Inc. IS-95, which uses DS-CDMA technology, has been deployed in US on trial basis. Bandwidth allotted is same as that of IS-54. Asymmetric modulation methods have been employed in the forward link (base-to-mobile) and the reverse link (mobile-to-base). Forward link employs BPSK with

Walsh orthogonal covering. Reverse link employs 64-ary orthogonal signaling. Both the links are spread at 1.2288 Mchips/sec. rate. A set of twenty 1.25 MHz bandwidth (approximately) CDMA channels can be used for either link. Qualcomm's QCELP (Qualcomm code excited LPC) speech coder is used for both the links. The speech coder outputs data at one of the four rates - 19.2, 9.6, 4.8 or 2.4 kbps depending upon the speech activity at a given instant in time. Rake receiver is used for equalization [1,4].

### 1.2.5 DECT (Digital European Cordless Telecommunication)

Like GSM, DECT is a Pan-European Standard deployed in many countries of Europe to provide an advanced cordless communication. Operating frequency range of DECT is 20 MHz between 1880 MHz and 1900 MHz. Ten carriers separated by 1.728 MHz are used, each carry twelve voice channels in TDMA format. DECT employs TDD (time division duplex) so that informations moves in both directions over the same carrier. In common with GSM, the modulation technique of DECT is GMSK. However the relative bandwidth of the Gaussian filter is wider (0.5 times the bit rate) than in GSM ( $BT = 0.3$ ). The bandwidth efficiency is 0.67 bps/Hz (1.152 Mbps in 1.728 MHz). Speech coder used is adaptive differential pulse code modulation (ADPCM) with a bit rate of 32 kbps [3,4].

## 1.3 PROBLEMS IN MOBILE COMMUNICATION

Since the communication between the mobile unit and the base unit is over RF link, one of the major problem encountered in the mobile communication is the problem of fading of the received signal. Since the antenna height of the mobile unit is lower than

it's typical surroundings, and the carrier frequency wavelength is much less than the sizes of the surrounding structures, multipath waves are generated. At the receiver, the sum of the multipath waves causes a signal-fading phenomenon. Since each path has a different path length, the time of arrival for each path is different at the receiver. If an impulse is transmitted, then by the time this impulse is received, it is no longer a impulse but rather a pulse with a spread width that we call as multipath spread or mean-square delay spread [1]. The measured data indicate that the delay spreads are different in different kinds of environment. Due to this signal spread in time domain inter symbol interference (ISI) becomes a major problem in mobile communication. Other problems include Doppler spectra due to vehicle motion, shadowing due to buildings and terrain which imposes a non-frequency selective, slowly changing fading upon the Rayleigh fading statistics and attenuation with distance which ranges from an inverse cubic law to inverse-fourth power law depending upon the terrain. To overcome ISI effects channel equalization techniques are used.

#### 1.4 CHANNEL EQUALIZATION

The most common type of channel equalizer used in practice to reduce ISI is a linear transversal filter with adjustable coefficients. On channels whose frequency response characteristics are unknown, but time-invariant, one can measure the channel characteristics and adjust the parameters of the equalizer, once adjusted, the parameters remain fixed during the transmission of the data. Such equalizers are called preset

equalizers. On the other hand, adaptive equalizers update their parameters on a periodic basis during the transmission of the data and, thus, they are capable of tracking a slowly time-varying channel response. The linear (adaptive) equalizers are very effective on channels such as wire line telephone channels, where ISI is not severe. Such equalizers are found to be unsuitable for mobile radio channels [4].

A decision feedback equalizer (DFE) is a nonlinear equalizer that employs previous decisions to eliminate the ISI caused by previously detected symbols on the current symbol to be detected. The DFE consists of two filters. The first filter, called as feed forward filter, is generally a fractionally spaced FIR filter with adjustable tap coefficients. Second filter called as feedback filter, is implemented as an FIR filter with symbol-spaced taps having adjustable coefficients. The input to the feedback filter is the set of previously detected symbols. The output of the feedback filter is subtracted from the output of the feedforward filter to form the input to the detector. Nonlinearity in DFE arises due to the nonlinear characteristics of the detector that provides the input to the feedback filter.

Although the DFE outperforms a linear equalizer, it is not the optimum equalizer from the viewpoint of minimizing the probability of error in the detection of the information sequence from the received signal samples. The optimum detector is a maximum likelihood symbol sequence detector which produces at its output the most probable symbol sequence for the given received sample sequence. An algorithm that implements maximum -

likelihood sequence estimation (MLSE) is the Viterbi algorithm.

As evident use of channel equalization make receiver design complex.

### **1.5 ENERGY DETECTION**

Energy detection is another possible method of combatting ISI. In the case of rapid fading, the non-coherent signaling detection operation is employed.

In order to obtain high data rates and reliable transmission on fading dispersive channels, such as mobile radio channels, one can use the diversity inherent in the available transmission bandwidth. A basic approach in extracting this diversity is to transmit pulses whose time duration and/or bandwidth cover many selective fades in time and/or frequency and to use energy detection for pulse discrimination [6].

Modulation techniques used is binary Frequency Shift Keying (FSK). Spectral energy in the vicinity of MARK frequency can be identified with MARK signals and energy around the SPACE frequency similarly identified with SPACE signals and the recognition is on the basis of frequency content, a factor which is not appreciably altered by the destruction of coherence over the pulse. Energy detection scheme used for mobile radio channels has been described in detail in Chapter 4. It is expected that design of receiver will become simpler using energy detection scheme.

### **1.6 STATEMENT OF THE PROBLEM**

To combat ISI encountered in mobile radio channels simulation of the Energy detection mobile system has been carried out. Same data rate as is used in GSM, i.e., 270.8 kbps is taken for the

simulation purpose. Multipath delay has been chosen as  $4.6 \mu\text{s}$  as at that time-delay power density spectrum falls off to 1/100th of its value. Typical channel impulse response used for suburban and urban area has been taken, which is used in designing the GSM system. Three IF bandwidths have been chosen for simulation and results are compared for the error probability of  $10^{-3}$ . The signals used are frequency-shift keyed rectangular RF pulses.

### 1.7 THESIS LAYOUT

A general fading channel model has been discussed in detail in Chapter 2. Various modifications of the general fading channel model like WSSUS fading channels, doubly spread channels, frequency-selective fading channels, time-selective fading channels etc. have been also discussed in Chapter 2. Chapter 3 includes characterization of mobile radio channels in terms of frequency-selective fading and time-selective fading. It also includes mobile mean path loss and shadowing. Simulation details including tapped delay line model used for simulation of channel are given in Chapter 4. Simulation results are also included in this chapter. Conclusions and suggestions for future work are included in Chapter 5.



## CHAPTER 2

### FADING CHANNELS

In various types of communication systems, the communication channel is modeled as a linear time-invariant system whose transfer function consists of a frequency-independent magnitude, less than unity, proportional to the propagation loss and a delay term proportional to the propagation delay between the channel modulator and the channel demodulator. In addition to this, the channel is usually considered to be corrupted by the Additive White Gaussian Noise (AWGN). Although this simple AWGN model is quite accurate for channels such as deep space communication channels, it is overly simplified model for a number of radio channels including microwave communication beyond the line of sight achieved via the tropospheric scatter, high frequency long distance communications achieved via ionosphere and mobile communication.

In these channels the received signal undergoes a process known as 'fading'. A fading channel may exhibit such properties as frequency selective response, intersymbol interference (ISI) in digital communications, spreading of the signals in the frequency domain, time varying amplitude response, or any combinations of these attributes.

Fading encountered over either a mobile radio channel or an HF ionospheric channel, for example, has been verified experimentally to be of two types : (1) short duration rapid fading over time spans of 1 sec or less, and (2) long duration

slow fading over time spans from 1 sec to 1 hour or longer. The statistics of the two fading processes are different.

The origin of the fading mechanism for the above mentioned fading channels may be traced to the scattering of an electromagnetic wave by a random medium. When an electromagnetic wave is scattered by a random medium, the scattered components can be resolved into in-phase and quadrature components whereas the instantaneous amplitudes of these two components are uncorrected. The inphase and the quadrature random processes collectively form a zero-mean complex Gaussian random process. If the random medium is single surface and is time-invariant, the received signal, after scattering, can be shown to have a Rayleigh distributed amplitude and a uniformly distributed phase (i.e., the signal is undergoing fading). So, for a sufficient number of scatterers, the scattering results in a zero mean complex Gaussian random process [2,7].

In the following sections a general fading channel model followed by WSSUS fading, doubly spread fading, time-selective fading, frequency-selective fading and nondispersive fading channel models are discussed.

## 2.1 GENERAL FADING CHANNEL MODEL

A general fading channel model is shown in Fig. 2.1. As shown in the figure, a signal is transmitted and scattered by a moving random medium which is assumed to be modeled as a layered scatterer, where each layer has an incremental thickness  $dr$ . [2]. Associated with each layer is a propagation delay  $\tau$ , which is in addition to the nominal propagation delay  $t_0$  between the

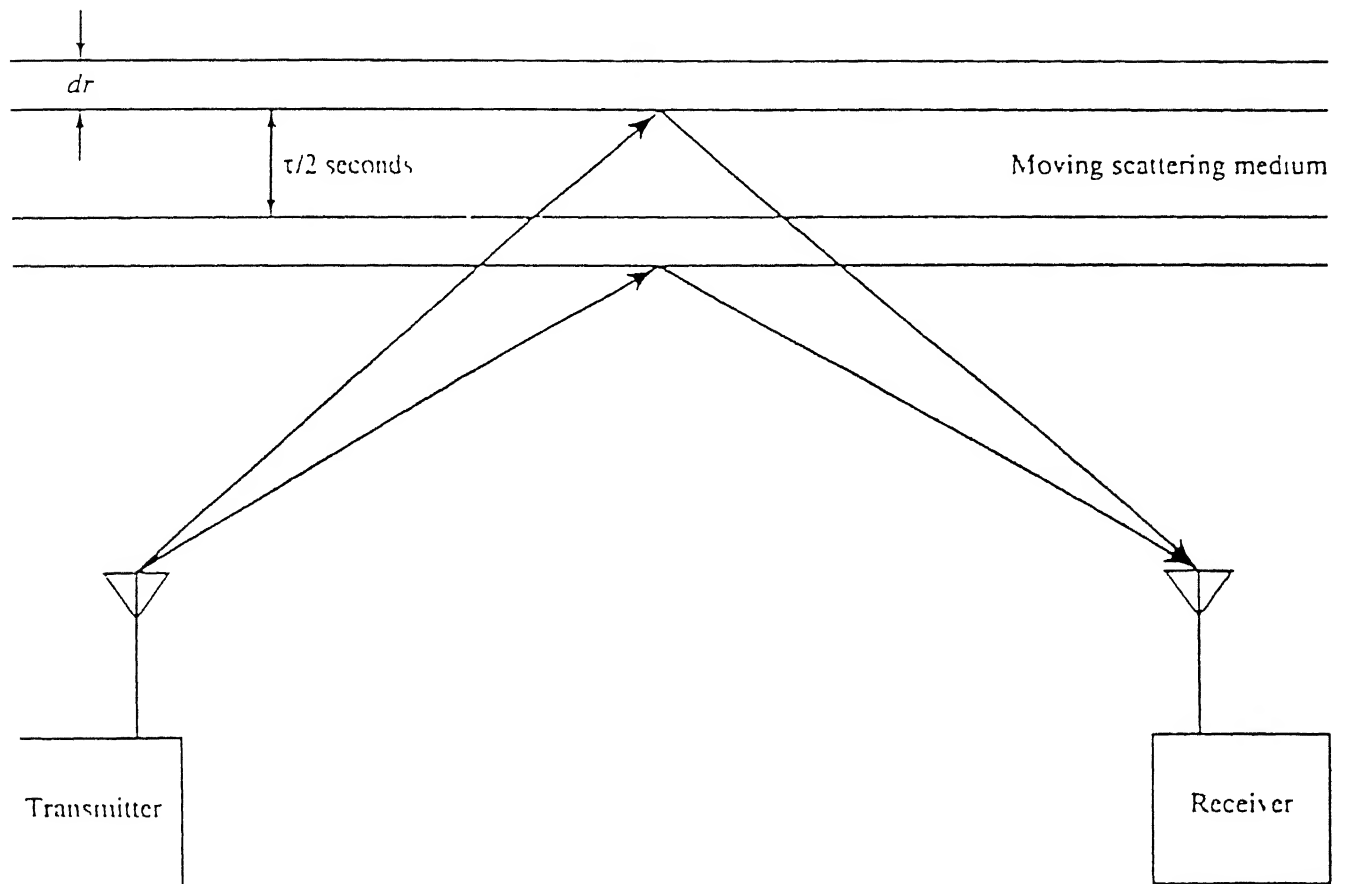


Fig. 2.1 Propagation model of a general fading channel

transmitter and the receiver.

The transmitted bandpass signal may be expressed as,

$$S_o(t) = \text{Re} \left[ u_o(t) e^{j2\pi f_o t} \right] \quad (2.1)$$

where  $u_o(t)$  is the complex envelope of the signal.

The received signal due to scattering from the layer is given by

$$S(\tau, t) = \text{Re} \left[ \beta(\tau, t-t_o) u_o(t-t_o-\tau) e^{j2\pi f_o (t-t_o-\tau)} \right] \quad (2.2)$$

where  $\beta(\tau, t)$  is the time-varying transmission coefficient for a wave scattering off a layer whose incremental propagation delay is  $\tau$ . The received signal is both time-varying due to the fact that the scattering volume was assumed to be moving and layer-dependent since the scattering medium was assumed to be able to be modeled as consisting of differential layers. Statistically  $\beta(\tau, t)$  has a Rayleigh-fading envelope and a uniformly distributed phase, both of which are time varying due to the presence of a moving random medium. Also the term  $\exp(j2\pi f_o \tau)$  may be absorbed into  $\beta(\tau, t)$  in eq. (2.2).

The total received signal is a superposition of the responses due to all the scattered layers :

$$S(t) = \int_{-\infty}^{\infty} \dot{S}(\tau, t) d\tau = \text{Re} \left[ \int_{-\infty}^{\infty} \beta(\tau, t_o) u_o(t-t_o-\tau) e^{j2\pi f_o (t-t_o)} d\tau \right] \quad (2.3)$$

### 2.1.1 Rayleigh and Rician Fading Channels

If the random medium is slowly-varying with time and can be modeled as consisting of a single layer, eq. (2.3) reduces to

$$S(t) = \text{Re} \left[ \beta u_o(t - t_o) e^{j2\pi f_o (t-t_o)} \right] \quad (2.4)$$

where  $\beta$  is a zero mean complex Gaussian random variable. Hence, the amplitude of the received wave is Rayleigh-distributed. Experimental evidence for the VHF and UHF mobile channel and HF ionospheric channel tends to support this prediction [8]; at the same time experimental data for some fading channels exhibits a Rician amplitude distribution. Rician fading is usually considered to be due to a specular component in the received path (i.e., the presence of a fixed non-random scatterer in the transmitter-receiver propagation path).

In this case eq. (2.3) may be modified to include a deterministic component in the received signal:

$$S(t) = \text{Re} \left[ A u_0(t-t_0) e^{j2\pi f_0(t-t_0)} + \int_{-\infty}^{\infty} \beta(\tau, t-t_0) u_0(t-t_0-\tau) e^{j2\pi f_0(t-t_0)} d\tau \right]$$

where  $A$  is the transmission coefficient associated with the specular path.

Many fading channels are not Rayleigh or Rician. Experimental data show that the amplitude of the received signal is log normally distributed in many instances. The deviations from a Rayleigh amplitude distribution may be due to an insufficient number of scatterers in a scattering layer to support the complex Gaussian random process hypothesis.

### 2.1.2 Correlation Functions

In determining the performance of communication systems over fading channels, second order statistical properties, i.e., autocorrelation and cross-correlation functions, are needed to

completely characterize the process.

To evaluate the autocorrelation function of the received signal two correlation functions are needed.

$$\hat{\Lambda}(\tau_1, \tau_2; t_1, t_2) \equiv \frac{1}{2} E \left[ \beta(\tau_1, t_1) \beta^*(\tau_2, t_2) \right] \quad (2.5)$$

$\hat{\Lambda}(\cdot)$ , given by eq. (2.5), is defined to be the space-time cross-correlation function (or simply the correlation function) of the fading process. One other correlation function associated with the general fading channel model is the frequency-time cross-correlations functions, given by

$$R(f_1, f_2; t_1, t_2) \equiv \frac{1}{2} E \left[ H(f_1; t_1) H^*(f_2; t_2) \right] \quad (2.6)$$

$$\text{where } H(f; t) = \int_{-\infty}^{\infty} \beta(\tau, t) e^{-j2\pi f\tau} d\tau \quad (2.7)$$

is the Fourier transform of the equivalent lowpass impulse response  $\beta(\tau, t)$  for the channel. Also from eq. (2.6) and (2.7).

$$R_F(f_1, f_2; t_1, t_2) = \int_{-\infty}^{\infty} \int_{-\infty}^{\infty} \hat{\Lambda}(\tau_1, \tau_2; t_1, t_2) e^{j2\pi(f_1\tau_1 - f_2\tau_2)} d\tau_1 d\tau_2 \quad (2.8)$$

which is the double Fourier transform of the space-time cross-correlation function.  $R_F(\cdot)$  is also known as the spaced-frequency spaced-time correlation function of the channel.

## 2.2 WSSUS FADING CHANNELS

The wide-sense stationary uncorrelated scattering (WSSUS) fading channel model is derived from the general fading model.

Some channels exhibit two types of fading : long-term fading and short-term fading. In short-term fading over these channels, short-term fading statistics are approximately stationary over time. Therefore, WSS channel model which is defined as a subclass of general fading channel model, is one whose correlation function

$R(\cdot)$  and  $\wedge(\cdot)$  are invariant under a time translation i.e. for WSS channel,

$$\wedge(\tau_1, \tau_2; t_1, t_2) = \wedge(\tau_1, \tau_2; t_1 - t_2) \quad (2.9)$$

$$R(f_1, f_2; t_1, t_2) = R(f_1, f_2; t_1 - t_2) \quad (2.10)$$

In many channels it can be assumed that the effect of scatterers in one differential layer is independent of the effect of the scatterers in all other differential layers, i.e., complex Gaussian process  $\beta(\tau, t)$  is independent of  $\beta(\sigma, t)$  for  $\sigma \neq \tau$ . The space-time cross-correlation function for such a channel is given by

$$\wedge(\tau_1, \tau_2; t_1, t_2) = \wedge(\tau_1; t_1, t_2) \delta(\tau_1 - \tau_2) \quad (2.11)$$

Channels whose  $\wedge(\cdot)$  satisfy eq. (2.11) are known as uncorrelated scattering (US) channels.

Channels which show both WSS and US channel characteristics are known as WSSUS channels. The space-time cross-correlation function  $\wedge(\cdot)$  for a WSSUS channel is given by:

$$\wedge(\tau_1, \tau_2; t_1, t_2) = \rho(\tau_1; t_1 - t_2) \delta(\tau_1 - \tau_2) \quad (2.12)$$

where  $\rho(\tau_1, t_1 - t_2) \equiv \wedge(\tau_1, \tau_2; t_1, t_2)$  for the special case of WSSUS channels. If  $\beta(\tau, t)$  is considered as a complex Gaussian process, wide-sense stationarity of  $\beta(\tau, t)$  implies strict-sense stationarity of  $\beta(\tau, t)$ .

Fortunately, the simplified WSSUS channel model characteristics are exhibited by most radio channels. Since, radio channel fading is characterized by the superposition of short-term fading on long-term fading. The short-term fading usually shows stationary characteristics while the long-term fading is often nonstationary depending on the interval of

interest. Bello has introduced the term Quasi-WSSUS (QWSSUS) to describe such a channel [9]. A QWSSUS channel has WSSUS channel characteristics over time intervals on the order of the duration of short-term fading.

### 2.3 DOUBLY SPREAD CHANNELS

It is a class of WSSUS fading channels. Doubly spread channels or doubly dispersive channels are so called because they spread both in time and frequency a signal transmitted through the channel [10].

For the doubly spread channel, the space-time cross-correlation function of the channel  $\Lambda(\cdot)$  is given by eq. (2.12). Most of the above relations can also be characterized in terms of a 'Scattering function'  $S_{DR}(\tau, f)$ , where  $S_{DR}(\tau, f)$  is the Fourier transform of  $\Lambda(\cdot)$ ,

$$S_{DR}(\tau, f) \equiv \int_{-\infty}^{\infty} e^{-j2\pi ft} \rho(\tau, t) dt \quad (2.13)$$

So  $S_{DR}(\tau, f)$  is the temporal Fourier transform of  $\rho(\tau, t)$ .

The following terms are defined in order to characterize the doubly dispersive channels [2]:

The 'mean delay' is defined as

$$m_R \equiv \frac{1}{2\sigma_b^2} \int_{-\infty}^{\infty} \int_{-\infty}^{\infty} \tau S_{DR}(\tau, f) d\tau df \quad (2.14)$$

The 'mean-square delay spread' is defined as

$$L \equiv \frac{1}{2\sigma_b^2} \int_{-\infty}^{\infty} \int_{-\infty}^{\infty} \tau^2 S_{DR}(\tau, f) d\tau df - m_R^2 \quad (2.15)$$

The 'mean-Doppler shift' is defined as

$$m_D \equiv \frac{1}{2\sigma_b^2} \int_{-\infty}^{\infty} \int_{-\infty}^{\infty} f S_{DR}(\tau, f) d\tau df \quad (2.16)$$

The 'mean-square Doppler spread' is defined as



$$B \equiv \frac{1}{2\sigma_b^2} \int_{-\infty}^{\infty} \int_{-\infty}^{\infty} f^2 S_{DR}(\tau, f) d\tau df - m_D^2 \quad (2.17)$$

$$\text{where } 2\sigma_b^2 = \int_{-\infty}^{\infty} \int_{-\infty}^{\infty} S_{DR}(\tau, f) d\tau df$$

An underspread channel is defined to be one for which  $BL < 1$

Similarly, an overspread channel is defined to be one for which,

$$BL > 1$$

The correlation (or coherence) time of a fading channel is defined as the time separation  $\tau_c$ , beyond which samples of the received signals are independent. The independence of time samples is implied if the correlation function of the envelope is zero. Since, the channel scattering process is assumed to be modeled as a zero-mean complex Gaussian process, given the transmitted signal, received signal is also a zero-mean complex Gaussian process. The correlation between the time samples of the received signal envelope is,

$$R_{TE}(t_1, t_2) \equiv \frac{1}{2} E[u(t_1)u^*(t_2)] = \int_{-\infty}^{\infty} \rho_T(\tau, t_1 - t_2) u_O(t_1 - \tau) u_O^*(t_2 - \tau) d\tau \quad (2.18)$$

$$\text{where } u(t) = \int_{-\infty}^{\infty} \beta(\tau, t) u_O(t - \tau) d\tau$$

By convention, the correlation time for the channel is chosen to be the smallest time separation  $\tau_c = t_1 - t_2$ , for which

$$R_{TE}(t_1, t_2) = 0 \quad (2.19)$$

Similarly, the correlation bandwidth of a fading channel is defined to be the frequency separation  $W_c$  beyond which samples of the Fourier transform of the received complex envelope are independent. As above, the Fourier transform of the received

envelope is also a complex Gaussian process. Thus, the independence of the frequency samples is implied if the correlation function of the Fourier transform of the received envelope is zero. The correlation between the frequency samples of the Fourier transform of the received signal envelope is given by

$$\begin{aligned} R_{FE}(f_1, f_2) &\equiv \frac{1}{2} E \left[ U(f_1) U^*(f_2) \right] \\ &= \int_{-\infty}^{\infty} \int_{-\infty}^{\infty} \int_{-\infty}^{\infty} \rho(\tau, t_1 - t_2) u_O(t_1 - \tau) u_O^*(t_2 - \tau) \cdot \\ &\quad e^{j2\pi(f_2 t_2 - f_1 t_1)} d\tau dt_1 dt_2 \end{aligned} \quad (2.20)$$

where  $U(f) = \int_{-\infty}^{\infty} \int_{-\infty}^{\infty} \beta(\tau, t) u_O(t - \tau) e^{-j2\pi f t} d\tau dt$  is the Fourier transform of the received envelope.

By convention the correlation bandwidth for the channel is chosen to be the smallest frequency separation  $W_c = f_1 - f_2$ , for which

$$R_{FE}(f_1, f_2) = 0 \quad (2.21)$$

Thus, the doubly Spread Channel is characterized in terms of channel correlation functions and the temporal Fourier transform of this quantity, the channel scattering function. Alternatively, the channel can also be characterized by the Fourier transforms of these quantities:

$$R_{DR}(\nu, t) \equiv \int_{-\infty}^{\infty} \rho(\tau, t) e^{-j2\pi \nu \tau} d\tau \quad (2.22)$$

and

$$P_{DR}(\nu, f) \equiv \int_{-\infty}^{\infty} S_{DR}(\tau, f) e^{-j2\pi \nu \tau} d\tau \quad (2.23)$$

where  $R_{DR}$  and  $P_{DR}$  are known as two-frequency correlation function

and the Doppler cross-power spectral density respectively.

It is often found that fading radio channels exhibits spreading predominantly in either the time or the frequency domains only. In such cases it is convenient to define subclasses of doubly spread channels having specific characteristics (also known as degenerate classes).

#### 2.4 TIME-SELECTIVE FADING CHANNELS

In the general fading channel model, scattering medium was assumed to be as randomly moving, layered volume of scatterers, each layer of which could be modeled as a complex Gaussian process. Now it will be assumed that the scattering medium can be modeled as a single layer of randomly moving scatterers. Such an assumption leads to the development of a class of channels known as time-selective fading channel. This model is also known as channel dispersive in frequency only, frequency-flat fading channel or Doppler spread channel.

If the signal  $S_o(t)$  is transmitted through scattering medium that can be modeled as a single layer, then the received signal is given by

$$S(t) = \text{Re} \left[ \beta(t-t_o) u_o(t-t_o) e^{j2\pi f_o(t-t_o)} \right] \quad (2.24)$$

where  $t_o$  is the propagation time between the transmitter and the receiver and  $\beta(t)$  is the time varying transmission coefficient due to the scattering medium. The above equation is obtained directly from the doubly spread fading channel model by ignoring the variable  $\tau$  of  $\beta$ , which is no longer important. The channel correlation function for time-selective fading channel is,

$$\rho(\tau, t-s) = \rho(0, t-s) \delta(\tau) \quad (2.25)$$

Since in eq. (2.24) the transmitted envelope  $u_o(t)$  is multiplied by  $\beta(t)$ , where  $\beta(t)$  is independent of frequency, therefore, the received envelope  $\beta(t)u_o(t)$  undergoes fading that is independent of frequency (i.e., the various frequency components of  $u_o(t)$  fade identically or frequency-flat fading). But  $\beta(t)$  is a time-varying function and as such acts to modulate the transmitted envelope of  $u_o(t)$  as shown in Fig. 2.2 for two different on-off pulse durations.

For short duration pulses, no effects are observed because of large bandwidth associated with them, while for longer duration pulses, the random modulation effects are readily apparent. This modulation process leads to spreading of the Fourier transform of the transmitted envelope in frequency domain-hence the origin of the term Doppler-Spread fading. Also  $\beta(\tau)$  is independent of  $\tau$ , the uncorrelated scattering condition of WSSUS channels is not really necessary in characterizing time-selective fading channels.

The scattering function for a time-selective fading channel is given by

$$S_{DR}(\tau, f) = S_D(0, f) \delta(\tau) = \delta(\tau) \int_{-\infty}^{\infty} e^{-j2\pi ft} \rho(0, t) dt \quad (2.26)$$

The term  $S_D(0, f)$  is known as the Doppler scattering function or the Doppler power spectrum of the channel. For a time-selective fading channel the mean delay and the mean-square delay spread are identically zero. Hence, these channels which exhibit spreading in frequency and not in delay, are often called as singly spread channels.

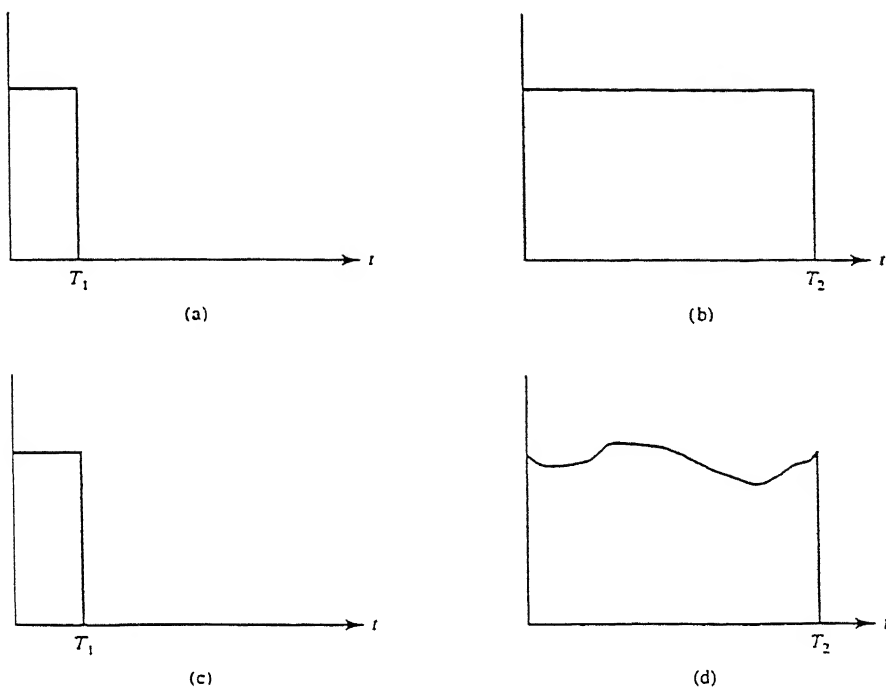


Fig. 2.2 Effect of transmitting a pulse over a time-selective fading channel : (a) transmitted short pulse; (b) transmitted long pulse; (c) received short pulse; (d) received long pulse

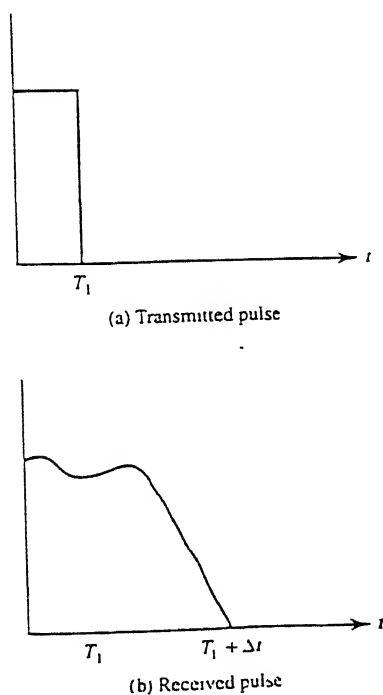


Fig. 2.3 Effect of transmitting a pulse over a frequency-selective fading channel

## 2.5 FREQUENCY-SELECTIVE FADING CHANNELS

The frequency-selective fading channels are also derived from the doubly spread channel by assuming that the scattering medium may be modeled as a fixed (nonmoving) volume consisting of differential layers. Individual scattering layers are uncorrelated.

The total received signal is given by

$$S(t) = \text{Re} \left[ \int_{-\infty}^{\infty} \beta(\tau) u_o(t-t_o-\tau) e^{j2\pi f_o(t-t_o)} d\tau \right] \quad (2.27)$$

Here  $\beta(\tau)$  is assumed to be zero mean complex Gaussian random variable with a Rayleigh distributed amplitude and a uniformly distributed phase.  $\beta$  is independent of the time variable  $t$  and is a function of incremental delay  $\tau$ . The effect of frequency selective fading channel on the envelope of an on-off pulse signal is shown in Fig. 2.3.

In the received envelope not only the amplitude is distorted by the random fading process, but the signal is spread in time to duration  $T_1 + \Delta t$ . Frequency selective fading channels are also known as time-flat fading channels [11], channels dispersive only in time and range or delay spread fading channels. The channel correlation function (also known as range scattering function or the multipath intensity or the power delay spectrum) for a frequency-selective fading channel is given by

$$Q(\tau) \equiv \rho(\tau, 0) \quad (2.28)$$

The range of values for which  $Q(\tau)$  is non-zero is known as the multipath spread or delay of the channel. The channel scattering function is given by

$$S_{DR}(\tau, f) \equiv Q(\tau) \delta(f) \quad (2.29)$$

The mean - Doppler shift and the mean - square Doppler spread for a frequency - selective fading channel are found to be identically zero.

## 2.6 NONDISPERSIVE FADING CHANNELS

For nondispersive fading channels it is assumed that the scattering medium is both fixed (nonmoving) and can be modeled as a single layer. This channel exhibits no spreading in frequency or time domain. It is also known as flat-flat fading channel or Rayleigh fading channel.

The received signal after passing through a fixed, single-layer scattering medium is given by

$$S(t) = \text{Re} \left[ \beta u_o (t - t_o) e^{j2\pi f_o (t - t_o)} \right] \quad (2.30)$$

Here,  $\beta$  is assumed to be a zero-mean complex Gaussian random variable.

The mean delay, mean-square delay spread, mean Doppler shift and mean-square Doppler spread for a nondispersive fading channel are all identically zero.

For exhibiting nondispersive fading

$$BL \ll 1 \quad (2.31)$$

i.e., nondispersive fading will occur in a doubly spread channel provided that the channel is underspread.

In Fig. 2.4 the hierarchy of fading channels are shown.

In chapter 3 a mobile radio channel, which is a specific example of the general fading channel model, is characterized in terms of its statistical properties.

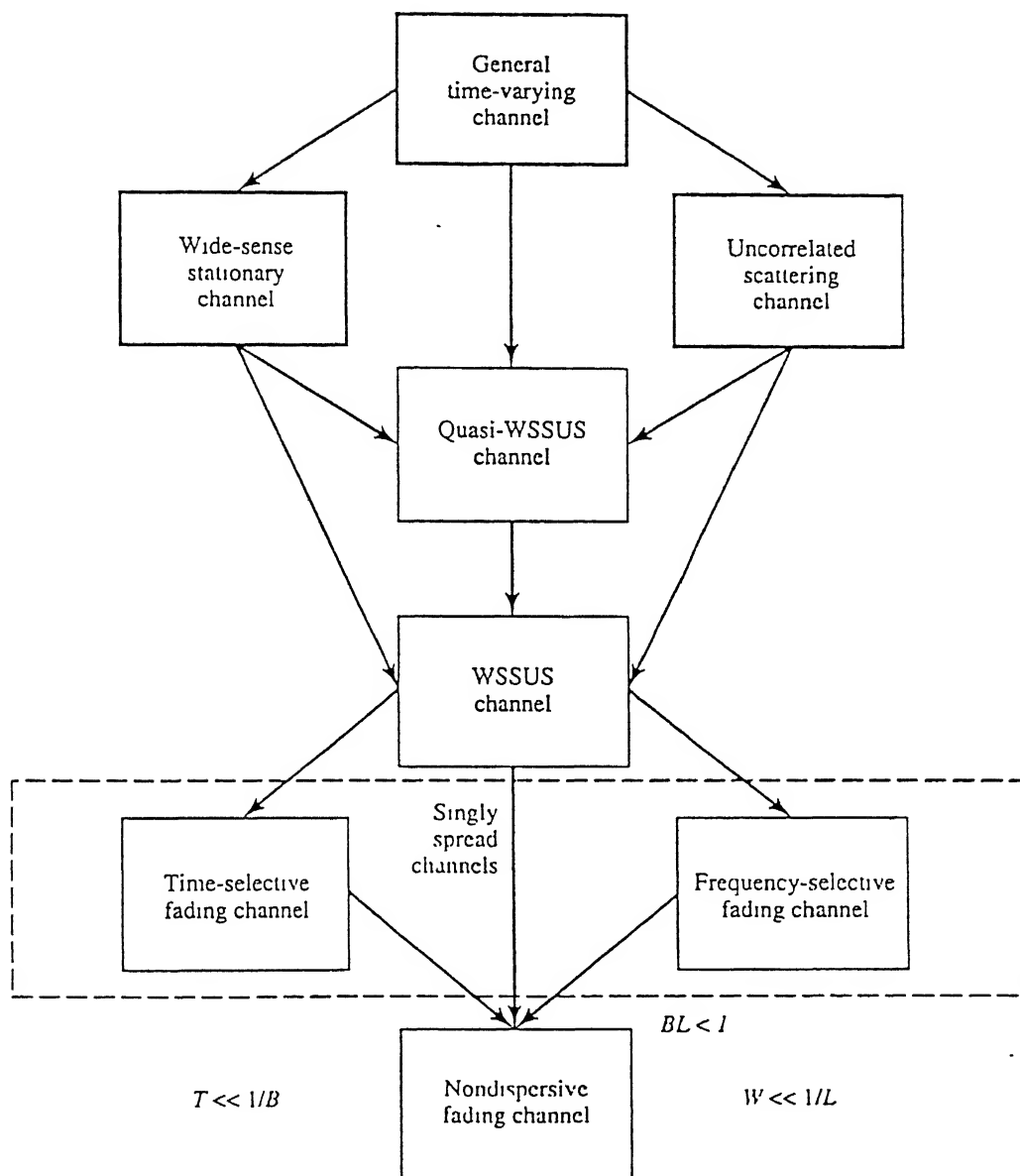


Fig. 2.4 Summary of hierarchy of fading channel models



## CHAPTER 3

### CHARACTERIZATION OF THE MOBILE RADIO CHANNEL

Mobile radio channel is a specific example of general fading channel model. Mobile radio channel exhibits the short term statistics of a doubly spread Gaussian wide sense stationary uncorrelated scattering channel. Mobile radio channel also exhibits long-term statistics that are distributed on the lognormal basis, which is caused by 'shadowing' by various obstacles in the direct path of the mobile radio wave. Because the presence or absence of the obstacles varies from location to location, the ability to communicate with any given mobile radio station may be statistically characterized in terms of a 'coverage reliability parameter'. Time-selective fading and frequency - selective fading, are found to be relevant to the mobile radio systems operating in cellular bands ( $\approx 800$  to  $900$  MHz) and in Personal Communication Service (PCS) bands ( $\approx 1.7$  to  $2.2$  GHz).

Time-selective fading and frequency-selective fading in mobile radio channels have been described in the following sections. Also mobile-radio path\* loss and shadowing effect have been discussed in this chapter.

#### 3.1 TIME-SELECTIVE FADING

Time-selective fading is present on both narrow band and wide band radio channels. The time-selective fading manifests itself as rapid variations of the received signal envelope as the mobile receiver moves through a field of local scatterers. The deviation of the fades from the median signal level is dependent on vehicle

speed and the operating frequency. Typical Rayleigh fading at 845 MHz for two vehicle speeds are shown in Fig. 3.1. [2].

A time-selective fading mobile radio channel can be characterized in terms of its Doppler power spectrum, correlation time, etc. as discussed in chapter 2. The statistical characteristics of the received signal for a mobile radio channel are also functions of the polarization of the antenna with respect to the received signal [12]. For vertical monopole case the auto-correlation function of the signal received by a mobile radio receiver corresponding to a constant, unmodulated carrier transmitted is given by

$$a(\tau) = J_0(2\pi f_m \tau) \quad (3.1)$$

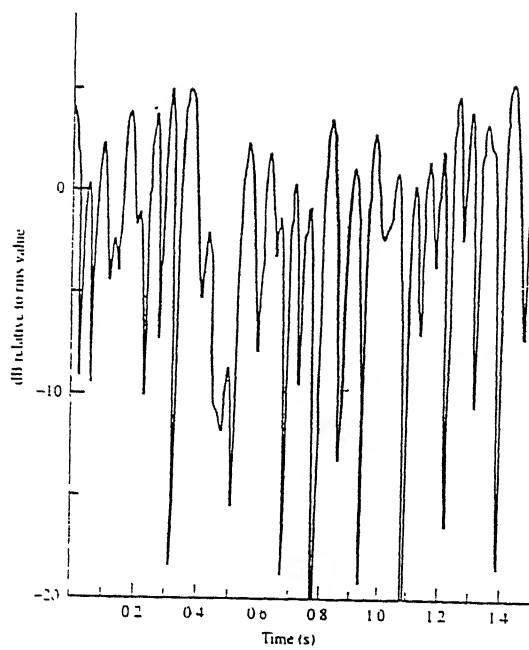
Where  $J_0(.)$  is the zero-order Bessel function of the first kind and  $f_m$  is the maximum Doppler frequency shift given by

$$f_m = \frac{v}{\lambda} = \frac{vf_o}{c} \quad (3.2)$$

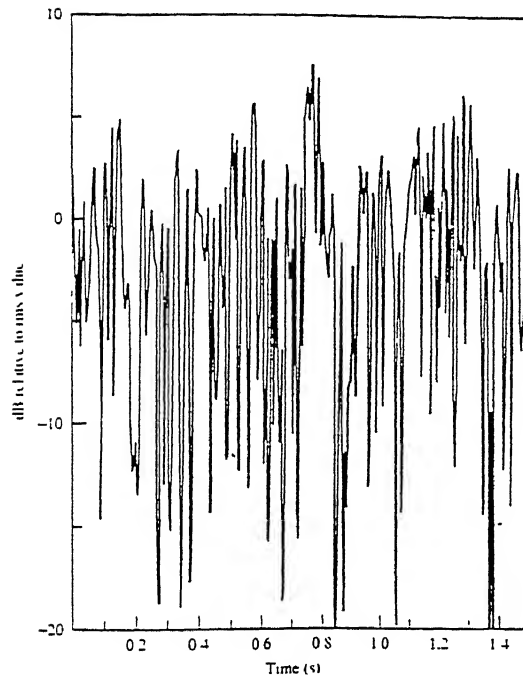
in which  $v$  is the speed (in m/s) of the vehicle,  $\lambda$  is the wavelength of the transmitted signal,  $c$  is the speed of light ( $= 3 \times 10^8$  m/s in vacuum), and  $f_o$  the frequency of the transmitted signal (in Hz). The Doppler spectrum is the Fourier transform of the autocorrelation function and is given by

$$S(f) = \begin{cases} \frac{1}{\pi f_m} \frac{1}{\sqrt{1 - (f/f_m)^2}} & |f| \leq f_m \\ 0 & \text{elsewhere} \end{cases} \quad (3.3)$$

The above equation is valid only for vertical monopole antennas and scatterers uniformly distributed around the antenna. The correlation (coherence) time of this channel is usually

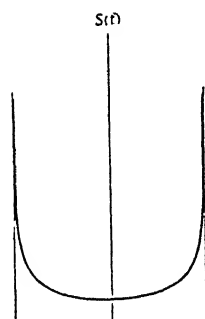


(a)



(b)

Fig. 3.1 Typical Rayleigh Fading at 845 MHz : (a) vehicle speed is 10 mph; (b) vehicle speed is 25 mph.



assumed to be given by

$$\tau_c = \frac{1}{2f_m} \quad (3.4)$$

The term 'normalized Doppler' is defined to be the product of the maximum Doppler frequency and the symbol duration of the transmitted signal. It can be shown that [8] for a vertically polarized monopole in a Rayleigh-fading mobile radio environment, the duration of a fade, defined to be the average duration of a fade below a given threshold  $A$ , is given by

$$\bar{t} = \frac{\lambda}{\sqrt{2\pi} VR} (e^{R^2} - 1) \quad (3.5)$$

where  $R = \frac{A}{\sqrt{2\sigma^2}}$

in which  $2\sigma^2$  is the average power of the received signal.

The plot of Doppler Spectrum for a mobile radio channel is shown in Fig 3.2

### 3.2 FREQUENCY-SELECTIVE FADING

In addition to exhibiting time-selective fading, the mobile radio channels also exhibit frequency-selective fading as described in the previous chapter. Frequency-selective fading may be characterized in terms of the mean delay and mean-square delay spread of the channel. For discrete multipath arrival times terms like mean excess delay, rms delay spread, and maximum excess delay are often used [13].

Let  $Q(\tau_k)$  denote the average power delay profile or delay power density spectrum, where  $\tau_k$  is the propagation delay from the transmitter to the receiver, then

$$\text{mean excess delay} = d_m = \frac{\sum \tau_k Q(\tau_k)}{\sum Q(\tau_k)} - \tau_A \quad (3.6)$$

where  $\tau_A$  is the first arrival delay. Similarly

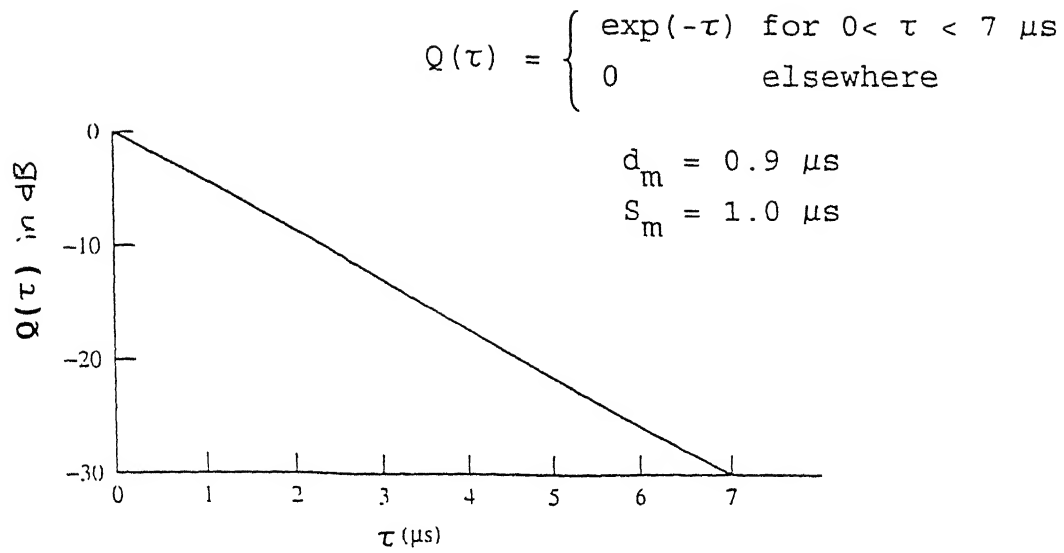
$$\text{rms delay spread} = S_m = \left[ \frac{\sum (\tau_k - \tau_A)^2 Q(\tau_k)}{\sum Q(\tau_k)} \right]^{1/2} \quad (3.7)$$

$$\text{and maximum excess delay} = \max (\tau_k - \tau_A) \quad (3.8)$$

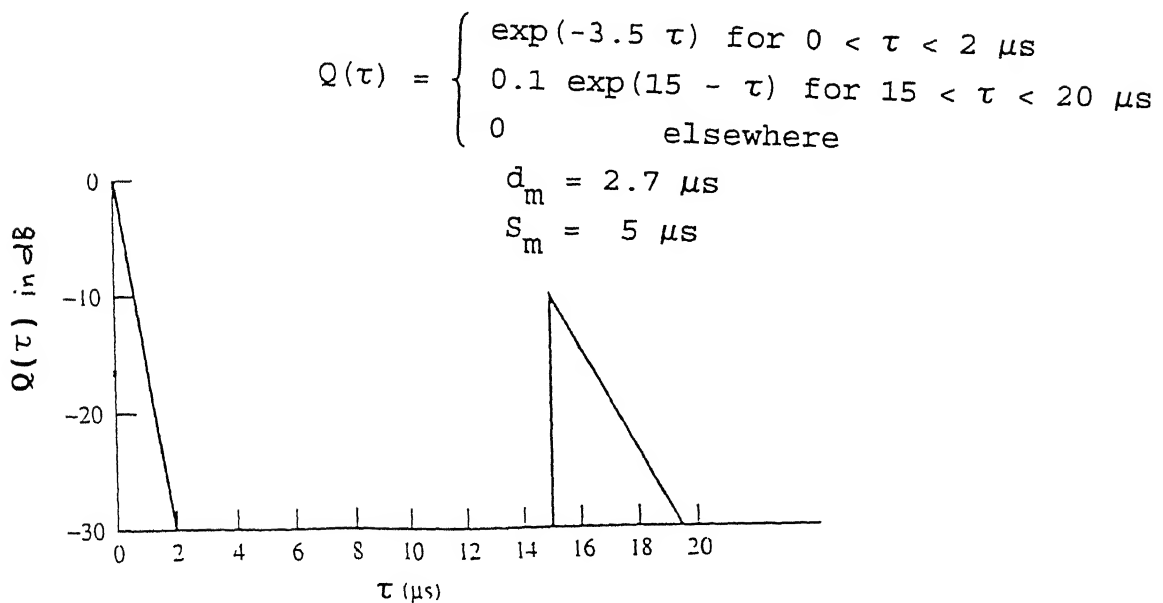
For urban terrain, the rms delay spread and maximum excess delay spread are of the order of 1 to 3  $\mu\text{s}$  and 3 to 6  $\mu\text{s}$  respectively. For suburban terrain these values vary from 0.1 to 1  $\mu\text{s}$  and 1 to 4.5  $\mu\text{s}$  respectively. For hilly terrain these values vary from 6 to 7  $\mu\text{s}$  and 20 to 35  $\mu\text{s}$  respectively [2].

In characterizing the mobile radio channels it is often necessary to specify power delay profile of the channel. Because the power delay profile is location dependent, so it becomes a difficult task to specify it. In 1986, a Scientific study group in Europe specified several average power delay profiles that modeled the mobile radio channel at 900 MHz quite well and were in fact used later in specifying the performance of the GSM digital Cellular System. Fig. 3.3 gives two of these profiles for the typical urban environment and the hilly terrain environment. Power delay profile for suburban and urban area has been used in the simulation reported in the next chapter.

Although both of these average power delay profiles are decaying exponentially with respect to delay indicating a minimum phase channel characteristic (i.e., channel impulse response decays as time increases), but, non-minimum phase channels can also exist in the mobile radio environment [2].



(a)



(b)

Fig. 3.3 Average Power Delay profiles : (a) typical delay profile for suburban and urban areas; (b) typical delay profile for hilly terrain.

### 3.3 MOBILE RADIO PATH LOSS

In free space, path loss for radio waves is of the form  $A(f)d^{-2}$ , where  $A(f)$  is a function of frequency, antenna gain, etc. and  $d$  is the distance between the transmitter and the receiver. But, in mobile radio environment, propagation is often not line-of-sight and the path loss is not equal to the free space path loss. Factors affecting the mean path loss include base and mobile antenna heights, operating frequency, the presence or absence of buildings, trees and foliage between the transmitter and the receiver, various ducting effects dependent on atmospheric condition, the presence or absence of the localized reflectors or absorbers etc.

To predict the mean path loss Hata model is [14] found suitable for relatively tall base station antennas (30 to 300 m) and frequencies less than 1.5 GHz. This model is of the form  $A+B \log_{10} d$  (in dB), where  $A$  and  $B$  are functions of frequency and height, and  $d$  is the distance between the transmitter and the receiver. The Hata model predicts mean path loss as a functional of the form  $Kd^{-r}$ , where  $r$  ranges from 2 to 4. This form of propagation loss model can simplify calculation for cell coverage reliability. A modified version of Hata model [2] is also obtained which is applicable to low base station antenna heights and over the frequency range 1.5GHz to 2 GHz. Again this propagation path-loss model is of the form  $Kd^{-r}$ .

### 3.4 SHADOWING

In addition to the short term statistics of the mobile radio channel, which led to the time-selective fading and the

frequency-selective fading, the presence of location-dependent obstacles leads to long-term fading or shadowing. Although shadowing results in a time-varying received signal, this phenomenon is unlike the time-selective fading, as vehicle speed is not a factor in determining the fading statistics. Extent of shadowing is determined by the nature of terrain surrounding the base and the mobile antennas, as well as the respective antenna heights with respect to the terrain. Since obstacles in the propagation path between the base and the mobile antennas lead to shadowing, simply moving the mobile location will usually change the effects of shadowing.

Shadowing may be modeled as a multiplicative, slowly time-varying random process. Hence, if the lowpass-equivalent transmitted signal is given by  $u_0(t)$ , the received signal  $r(t)$  in the absence of time-selective and frequency-selective is given by:

$$r(t) = A_m(t) u_0(t) \quad (3.9)$$

where  $A$  accounts for the antenna gains and the mean path loss between the transmitting antenna and the receiving antenna and  $m(t)$  is the random process due to shadowing which is generally assumed to be lognormally distributed. In the presence of time and/or frequency selective fading, eq. (3.9) still holds true with  $u_0(t)$  replaced by a suitable term that includes the short-term fading effects.

In Chapter 4, simulation of an energy detection scheme for mobile radio channel is discussed.



## CHAPTER 4

## SIMULATION OF FSK ENERGY DETECTION MOBILE SYSTEM

In section 4.1 energy detection scheme is explained. Simulation of energy detection scheme is given in section 4.2. Simulation results and discussion of the results are given in sections 4.2 and 4.3 respectively.

**4.1 Energy Detection:**

In order to obtain reliable transmission over fading dispersive channels such as mobile fading channels clever use must be made of all the diversity inherent in the available transmission bandwidth. A basic approach to extract this diversity, is to transmit pulses whose time duration and/or bandwidth covers many selective fades in time and/or frequency and to use energy detection for pulse discrimination [15].

In the case of high-speed digital transmission, the pulse width is very small compared to the fading time constant or the coherence time of the channel, and thus time diversity may not be achieved by a single pulse. The only way to extract the diversity available in the transmission bandwidth is to have the bandwidth of the pulse larger than the coherence bandwidth of the channel, i.e., there are several independent fading elements (also known as degree of freedom) in one transmitted pulse. This requires that the signal bandwidth must be wide, which implies that the transmitted pulse should be short.

The basic model of the energy detection scheme is shown in Fig. 4.1. In the system discussed here the various possible MARK-SPACE frequencies (corresponding to bit 1 and 0 respectively) change pairwise with time in a cyclical pattern and the symbol decision is based on the amount of energy in a time

gate positioned at the output of the filters centered on the two possible frequencies corresponding to any time slot. The time gates are chosen so that most of the energy of the transmitted pulse is located within the time gate. Thus, the width of the gate is a function of transmitted pulse width and the channel multipath spread or mean-square delay spread. Enough distinct MARK and SPACE frequencies must exist so that the intersymbol interference due to frequency-selective fading can be made negligible by making the MARK-SPACE frequency allocations for successive pulses occupy different carrier frequencies in a stairstep fashion, i.e., there should be a sufficient number of MARK and SPACE frequencies so that a frequency is not repeated until the possible intersymbol interference due to the last transmission at that frequency has died out [6]

A 3 frequency-pair FSK signaling sequence is shown in Fig 4.2

The total allowable RF bandwidth is divided into two equal adjacent nonoverlapping frequency intervals called the MARK and the SPACE band. Each MARK and SPACE band is further divided into N equal subdivision, numbered sequentially from 1 to N in each band. The FSK transmission scheme utilized is to transmit at time  $t_I$ , for  $1 \leq I \leq N$  a gated sine wave at either frequency  $M(I)$  or  $S(I)$ , depending on whether a MARK or a SPACE is desired, and for  $I > N$ , selecting the allowable frequency pairs on a modulo N basis. The pulse width T is chosen such that

$$T \leq t_{I+1} - t_I \quad (4.1)$$

For N-frequency pairs, it takes a minimum of  $N(t_{I+1} - t_I)$  seconds before a particular frequency pulse is retransmitted. If multipath spread were limited to L seconds, then

$$N(t_{I+1} - t_I) \geq L \quad (4.2)$$

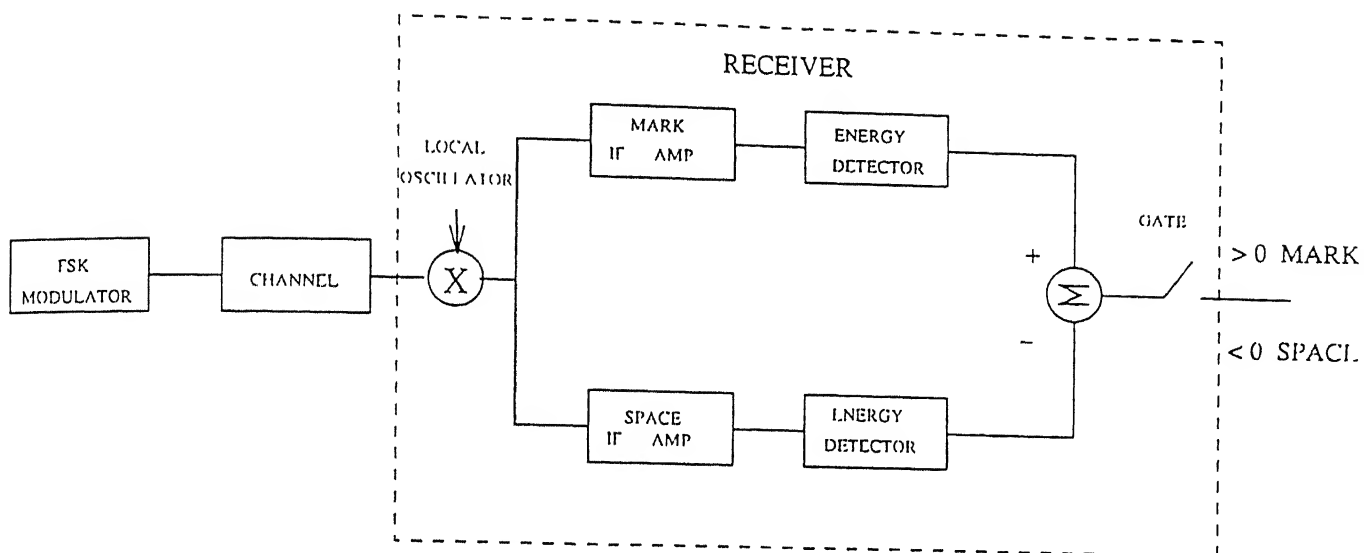


Fig. 4.1 Energy detection FSK System

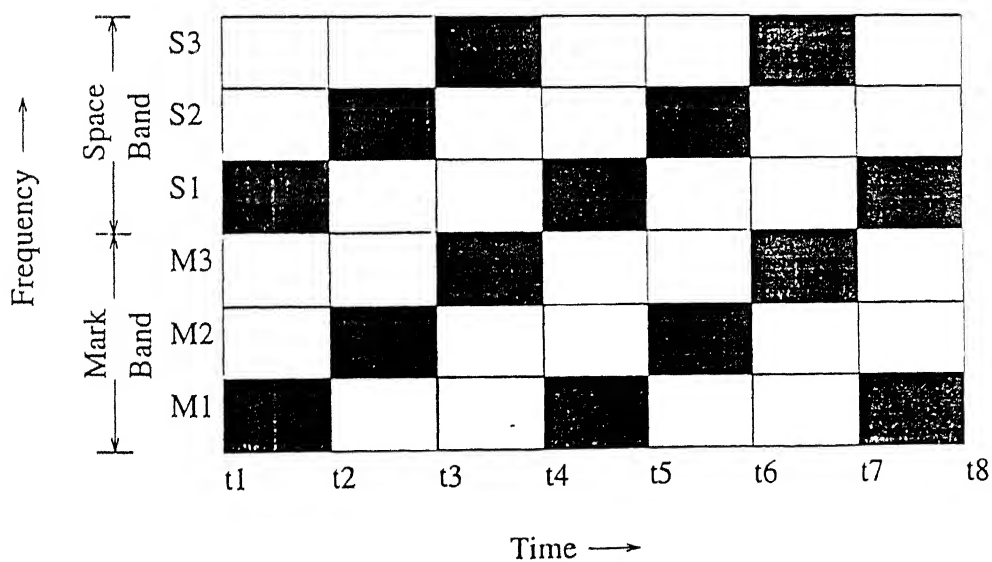


Fig. 4.2 3-Frequency-Pair FSK Signaling Sequence

in order for there to be no intersymbol interference. Furthermore if  $W$  is the bandwidth of the transmitted pulse and  $B_{\max}$  is the maximum allowable bandwidth, then it is necessary that

$$2NW \leq B_{\max} \quad (4.3)$$

## 4.2 Simulation of Energy Detection Scheme

### 4.2.1 Tapped Delay Line model of the Channel

Frequency-selective fading channel can be modeled as tapped delay line. Time-selective fading is not considered, because the Doppler shift caused by it is negligible (see sec. 3.1) as compared to the pulse bandwidth. Moreover for normal speed of mobile the shadowing effect is assumed to be the same for all the time slots and frequency bands, i.e., shadowing varies too slowly to affect demodulation and is not frequency-selective [16,17]. Path loss caused by shadowing is assumed to be included in the mobile radio path loss.

The delay power density spectrum or the channel impulse response  $Q(\tau)$ , which is used to calculate the tap gain coefficients of tapped delay line model, presents a physical picture of the channel's time domain behaviour [9]. The area under  $Q(\tau)$  between  $\tau$  and  $\tau+d\tau$  is the percentage of received power due to path delays lying in the interval  $(\tau, \tau+d\tau)$ . Although  $Q(\tau)$  is not statistically stationary, but for the short-time fluctuations of the channel  $Q(\tau)$  is assumed to be time independent. The delay power density spectrum used in the simulation is given in Fig. 3.3(a), which is redrawn in Fig. 4.3 using absolute scale.

Assume that the channel responds to frequencies within the interval  $f_i - W_i/2 < f < f_i + W_i/2$  and let  $z(t)$  and  $w(t)$  be the complex channel input and output respectively, then

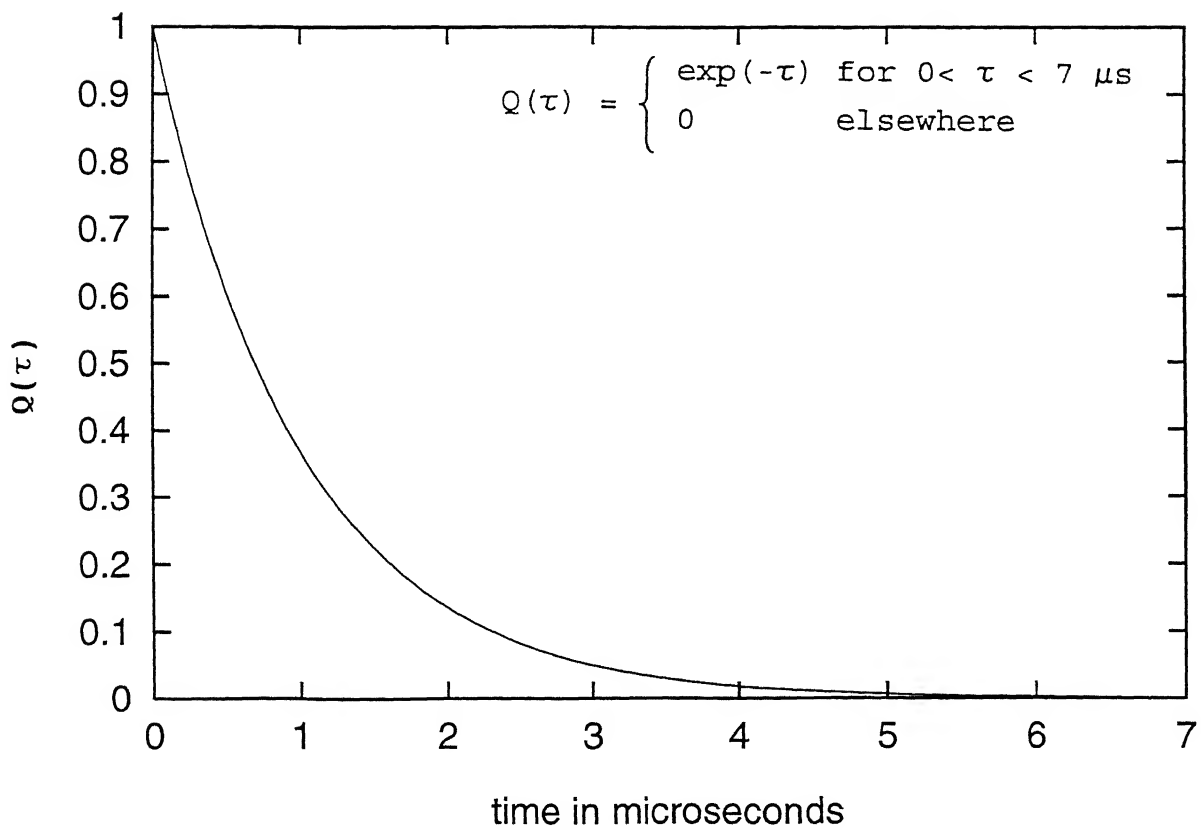


Fig. 4.3 Average Power Delay Profile for suburban and urban areas (in absolute scale)

$$w(t) = \int_{-\infty}^{\infty} z(t-\tau) \beta(\tau, t) d\tau \quad (4.4)$$

where  $\beta(\tau, t)$  is the time-varying impulse response of the channel and as such is the complex gain associated with path delays in the interval  $(\tau, \tau+d\tau)$ .

Using sampling theorem, samples of  $\beta(\tau, t)$  at time intervals  $1/W_i$  apart expressed as [6].

$$\beta(\tau, t) = \sum_{n=-\infty}^{\infty} \beta\left(\frac{n}{W_i}, t\right) \exp\left[j2\pi f_i \left(\tau - \frac{n}{W_i}\right)\right] \text{sinc} \left[W_i \left(\tau - \frac{n}{W_i}\right)\right] \quad (4.5)$$

From eq. (4.4) and (4.5),  $w(t)$  is expressed as

$$w(t) = \int_{-\infty}^{\infty} \left\{ \sum_{n=-\infty}^{\infty} \frac{1}{W_i} \beta\left(\frac{n}{W_i}, t\right) W_i \exp\left[j2\pi f_i \left(\tau - \frac{n}{W_i}\right)\right] \cdot \text{sinc} \left[W_i \left(\tau - \frac{n}{W_i}\right)\right] z(t-\tau) \right\} d\tau \quad (4.6)$$

$$= \sum_{n=-\infty}^{\infty} \beta_n(t) \int_{-\infty}^{\infty} \left\{ z(t-\tau) W_i \exp \left[ j2\pi f_i \left( \tau - \frac{n}{W_i} \right) \right] \cdot \text{sinc} \left[ W_i \left( \tau - \frac{n}{W_i} \right) \right] \right\} d\tau \quad (4.7)$$

$$\text{Where } \beta_n(t) \equiv \frac{1}{W_i} \beta\left(\frac{n}{W_i}, t\right) \quad (4.8)$$

The integral in eq. (4.6) is the convolution of the input with the time functions,

$$W_i \exp [j2\pi f_i (t-n/W_i)] \text{sinc} [W_i (t - n/W_i)]$$

which corresponds to passing the input signal through the band limited filter

$$\text{rect} ([f-f_i]/W_i) \exp [-j2\pi n f/W_i]$$

This results in the tapped delay line model shown in Fig.

4.4. The total number of taps in the delay line is given by

$$\begin{aligned} M_{\text{TAPS}} &= \left( \tau_{\max} - \tau_{\min} \right) \bigg/ \frac{1}{W_i} \\ &= W_i (\tau_{\max} - \tau_{\min}) \\ &= W_i L \end{aligned} \quad (4.9)$$

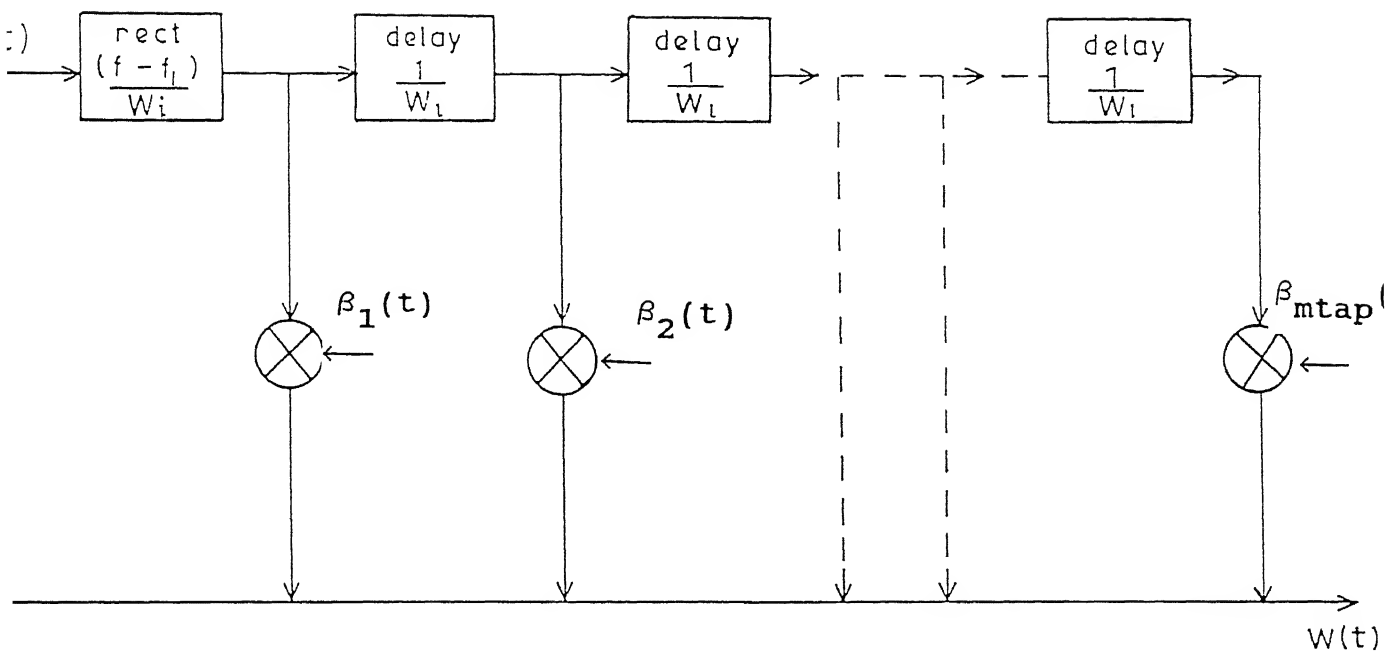


Fig. 4.4 Tapped Delay Line Channel Model

where  $L = (\tau_{\max} - \tau_{\min})$  is the multipath delay or mean-square delay spread.

For the special case of the WSSUS channel with input frequency constraints, the input band-limiting filter can be incorporated into the taps, with the result that the correlation properties of the taps can be shown to be [9]

$$\begin{aligned} < \beta_n^* (t) \beta_m (t + \xi) > \\ &= \int \exp [j2\pi f_i \left( \frac{n-m}{W_i} \right)] \operatorname{sinc} \left[ W_i \left( \tau - \frac{n}{W_i} \right) \right] \cdot \\ &\quad \operatorname{sinc} \left[ W_i \left( \tau - \frac{m}{W_i} \right) \right] Q(\xi, \tau) d\tau \end{aligned} \quad (4.10)$$

Where  $Q(\xi, \tau)$  is the channel correlation function. For  $\xi = 0$ , we define

$$Q(0, \tau) = Q(\tau) \quad (4.11)$$

If  $Q(\xi, \tau)$  changes little for changes in  $\tau$  in the order of  $1/W_i$ , one can have the approximation.

$$< \beta_n^* (t) \beta_m (t + \xi) > \approx \begin{cases} 0, & m \neq n \\ \frac{1}{W_i} Q \left( \xi, \frac{n}{W_i} \right), & m = n \end{cases} \quad (4.12)$$

Thus the tap gains are uncorrelated Gaussian random variables, the variance of which are proportional to  $Q(0, n/W_i)$ , the delay power density spectrum evaluated at time  $n/W_i$ . Tap gains are given by

$$\beta_n = (a_n + jb_n) \sqrt{\frac{Q(0, n/W_i)}{2W_i}} \quad (4.13)$$

where  $a_n$  and  $b_n$  are independent Gaussian random variables with zero mean and unity variances.

#### 4.2.2 Signal Flow Diagram

The simulated signal flow diagram is shown in Fig. 4.5.

In the Figure tapped delay line model of the channel is generated as discussed in Sec. 4.2.1. The transmission of the signal over the channel is simulated by the convolution of the



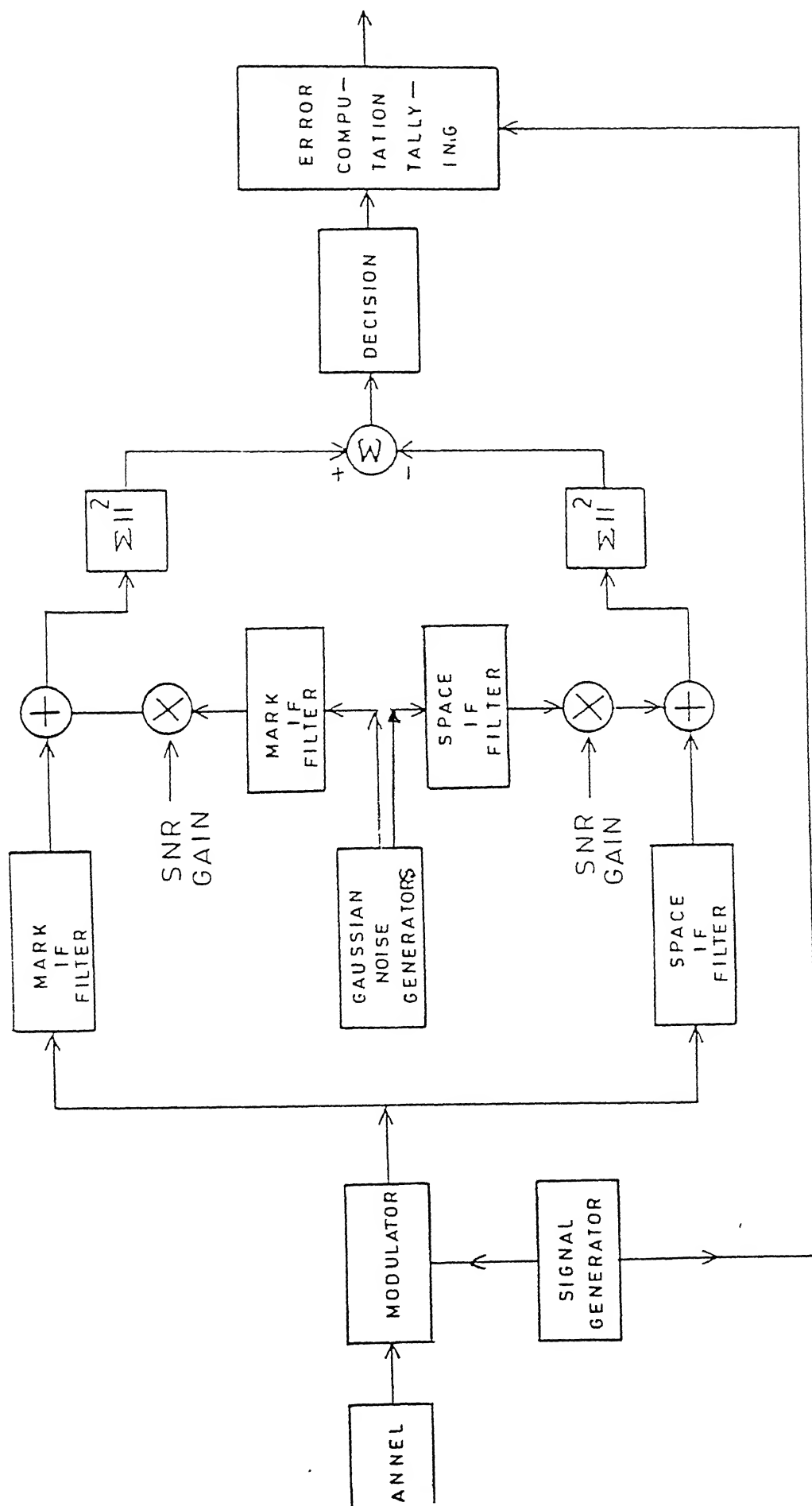


Fig. 4.5 Signal Flow Diagram of the Simulated System

signal with the channel in the modulator block. Each signal is tested over a new channel.

As the simulation is performed using complex signals, it is necessary to process them in complex filters. Briefly the complex filter has a passband of width  $W$  centered about some nonzero frequency  $\Omega$ . Unlike conventional real filters, there is no corresponding passband centred about  $-\Omega$ . A technique for realising the digital versions of these filters is fully discussed in [18]. To include the effects of receiver noise Gaussian white noise is filtered in complex MARK and SPACE filters separate from the (complex) signal MARK and SPACE filters. The filtered noises are then multiplied by a weighting factor and added to the respective filtered signals to form a sampled sequence of signal plus noise. The effect of different SNRs on a received signal is algebraically found by changing the weighting factor. The sample sequences are squared and summed to simulate energy detection. At each gate time, a MARK-SPACE decision is made and, based on the knowledge of the transmitted signal, it is noted whether or not an error has been made.

#### 4.2.3 Simulation Details

Data rate is taken as 270.8 Kbps, the same as used in GSM. Bit interval,  $T$ , is  $3.7\mu\text{s}$ . Multipath delay is taken to be  $4.6\mu\text{s}$ , because at this time the delay power spectrum reduces to 1/100th of its value. Gate width is chosen to be  $8.3\mu\text{s}$ , i.e., the sum of bit interval and multipath delay. Sampling of the channel is carried out at 25 MHz so that the approximation of eq. (4.12) is held. Total numbers of taps used are 116. Three IF bandwidths are chosen corresponding to  $2/T$ ,  $1.5/T$  and  $1/T$ . Complex Butterworth filter of the fourth order is used in simulation. For

each iteration different seed is used for generating the normally distributed random numbers.

### 4.3 SIMULATION RESULTS

By changing the weighting factor in the filtered Gaussian noise, the simulations runs have been carried out for different SNRs. The results of simulation runs for different received SNRs have been plotted in Fig. 4.6. The probability of the error is just the probability that the energy of signal plus noise is exceeded by the energy of noise. Fig. 4.6 includes three curves corresponding to three IF band widths chosen. In the simulation we are looking for the probability of error of the order of  $10^{-3}$ , which is found to be adequate for voice transmission in mobile radio communication [19,20]. Finally, ensemble average is taken over the probabilities of error obtained for more than ten runs in each case for calculating the average probability of error.

### 4.4 DISCUSSION OF THE RESULTS

Probability of error ( $P_e$ ) for three IF bandwidths for different SNRs has been shown in Fig. 4.6. As evident from the figure IF bandwidth  $2/T$  gives minimum  $P_e$  for a given SNR. But the bandwidth it occupies is large (540 KHz) as compared to IF bandwidths of  $1.5/T$  (405 KHz) and  $1/T$  (270 KHz). For the  $10^{-3}$  probability of error, the signal power is increased by 0.5 dB while going from  $2/T$  IF bandwidth to  $1.5/T$  IF bandwidth and 2 dB while going from  $1.5/T$  IF bandwidth to  $1/T$  IF bandwidth. So bandwidth and signal power trade-off is possible. Coherence bandwidth of the channel is  $1/L$  (where  $L = 4.6 \mu s$ ), i.e., 217.4 KHz. So, for 540 KHz bandwidth, we are getting effective diversity of the order of 2.48 [21] and for 405 KHz and 270 KHz bandwidth the effective diversity obtained is of the order of 1.86 and 1.24 respectively.

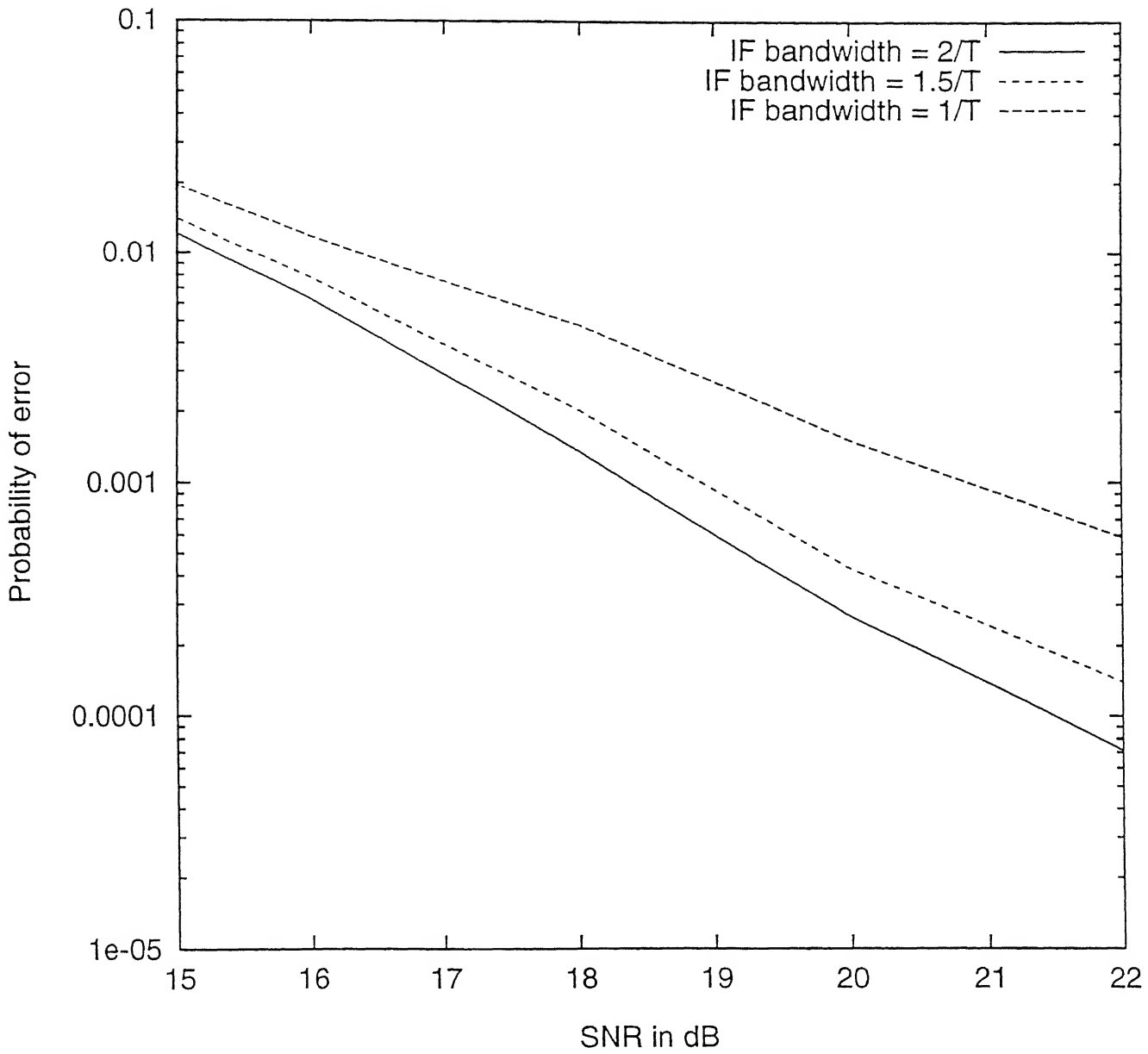


Fig. 4.6 Measured Error Probability of Simulated FSK energy detection Mobile System

## CHAPTER - 5

## CONCLUSION

Simulation of an FSK energy detection mobile system has been carried out. Frequency selective fading channel was modeled as tapped delay lines. Data rate chosen is 270.8 kbps, which is the same as used in GSM. In 270.8 kbps data rate 8 users are time multiplexed. Bandwidth occupied for 3-frequency pair FSK signaling sequence is 3.24 MHz, 2.43 MHz and 1.62 MHz for  $2/T$ ,  $1.5/T$  and  $1/T$  IF bandwidths, respectively. For total 25 MHz bandwidth available for the mobile system, this scheme can accommodate roughly 64, 80 and 120 users respectively by repeating such patterns. Each user can be assigned a time slot number and a frequency band number for identification purpose.

For accommodating 120 users signal power has to be increased 2.5 dB as compared to accommodating 64 users. Equalization of the received pulses is not necessary which simplifies the receiver design. But a price is paid in terms of accommodating less number of users. This system could be proposed to be used in an area where the number of active users is small like in rural areas or remote areas. This system can be compared with DECT (as discussed in chapter 1) which works with 20 MHz bandwidth and accommodates 120 active users, since in the proposed system 120 users can be accommodated while using 270 KHz IF bandwidth.

### 5.1 SUGGESTION FOR FUTURE WORK

Effect of adjacent channels noise may be investigated. Consequences of increased data rate for accommodating more users may also be evaluated. Effect of interference from the adjacent cells (cochannel interference) could be considered. The

performance of the energy detection scheme can be evaluated for bandwidth efficient schemes like minimum shift keying (MSK), Gaussian minimum shift keying (GMSK), etc. We have used Butterworth filter of the fourth order in simulation. The effect of higher or lower order filters can also be investigated in improving the performance of the system. Simulation may also be carried out by including the effects of mean path loss and shadowing.

## REFERENCES

1. William C.Y. Lee, "Mobile Cellular Telecommunication - Analog and Digital Systems", Second Edition, McGraw-Hill, Inc. 1995.
2. Roger L. Peterson, Rodger E. Ziemer, and David E. Borth, "Introduction to Spread Spectrum Communications", Prentice-Hall, 1995.
3. David J. Goodman, "Second Generation Wireless Information Networks", IEEE Transactions on Vehicular Technology, Vol. 40, No. 2, May 1991.
4. Jerry D. Gibson, "The Mobile Communications Handbook", CRC press, 1996.
5. Krister Raith, "Capacity of Digital Cellular TDMA Systems", IEEE Transactions on Vehicular Technology, Vol. 40, No. , May 1991.
6. P. A. bellow and Leonard Ehrman, :Performance of an Energy Detection FSK Digital Modem for Tropascatter Links", IEEE Transaction on Communicatin Technology, Vol. COM-17, No. 2, April 1969.
7. M. Schwartz, William R. Bennet and Seymour Stein, "Communication Systems and Techniques", McGraw-Hill, Inc., 1966.
8. William C. Jakes Jr., "Microwave Mobile Communications", John-Wiley and Sons, 1974.
9. P. A. Bello, "Characterization of Randomly Time-Variant Linear Channels", IEEE Transactions on Communication Systems, December 1963.

10. R.S. Kennedy, "Fading Dispersive Communication Channels", John-Wiley and Sons, 1969.
11. P. A. Bello and B.D. Ivelin, "The effect of Frequency-Selective fading on the Binary Error Probabilities of Incoherent and Differentially Coherent Matched Filter Receivers", IEEE Transactions on Communication Systems, June 1963.
12. M.J. Gans, "A power spectral theory of propagation in the mobile radio environment", IEEE Transactions on Vehicular Technology, Vol. VT-21, pp. 27-38, 1972.
13. Donald C. Cox, and Robert P. Leck, "Distribution of Multipath Delay Spread and Average Excess Delay for 910 MHz Urban Mobile Radio Paths", IEEE Transactions on Antenna and Propagation, Vol. AP-23, No. 2, March 1975.
14. M. Hata, "Empirical Formula for Propagation Loss in Land Mobile Radio Services", IEEE Transactions on Vehicular Technology, Vol. VT-29, pp. 317-325, August 1980.
15. Special Issue on Project West Ford, Proceedings IEEE, Vol. 52, May 1964.
16. Dider Verhulst, M. Mouly, and J. Szpirglas "Slow Frequency Hopping Multiple Access for Digital Cellular Radio Telephone", IEEE Transactions on Vehicular Technology, Vol. VT-33, No. 3, August 1984.
17. Ray W. Nettleton and George R. Cooper, "Performance of a Frequency - Hopped Differentially Modulated Spread-Spectrum Receiver in a Raleigh Fading Channel", IEEE Transactions on Vehicular Technology, Vol. VT-30, No. 1, February 1981.



18. Thomas H. Crystal and L. Ehrman, "The Design and Applications of Digital Filters with Complex Coefficients", IEEE Transactions on Audio and Electroacoustics, Vol. AU-16, No. 3, September 1968.
19. D.J. Goodman, P.S. Henry, and V. K. Prabhu, "Frequency-Hopped Multilevel FSK for Mobile Radio", The Bell System Technical Journal, Vol. 59, No. 7, September 1980.
20. Phillip D. Rasky, G.M. Chiasson, D.E. Borth and R.L. Peterson, "Slow Frequency-Hop TDMA/CDMA for Macrocellular Personal Communications", IEEE Personal Communications, Second Quarter, 1994.
21. R. S. Kennedy, and I.L. Lebow, "Signal design for dispersive channels", IEEE Spectrum, March 1964.